

Antiplane response of two scalene triangular hills and a semi-cylindrical canyon by incident SH-waves

Yang Zailin^{1†}, Xu Huanan^{2‡}, Hei Baoping^{1‡} and Zhang Jianwei^{1‡}

1. College of Aerospace and Civil Engineering, Harbin Engineering University, Harbin 150001, China

2. School of Resource Engineering, Longyan University, Longyan 364012, China

Abstract: Antiplane response of two scalene triangular hills and a semi-cylindrical canyon by SH-waves is studied using wave function expansion and complex function method. Firstly, the analytical model is divided into three parts, and the displacement solutions of wave fields are constructed based on boundary conditions in the three regions. Three domains are then conjoined to satisfy the “conjunction” condition at shared boundary. In addition, combined with the zero-stress condition of semi-cylindrical canyon, a series of infinite algebraic equations for the problem are derived. Finally, numerical examples are provided and the influence of different parameters on ground motion is discussed.

Keywords: scattering of SH-waves; scalene triangle hills; semi-cylindrical canyon; ground motion

1 Introduction

Demonstrated by domestic and international earthquake damage experience of a number of factors (earthquake source, propagation medium and path, site conditions and local terrain) that impact the ground motion, local terrain is the key one to cause surface earthquake damage or ground motion. Thus, estimating the influence of local terrain on seismology is a growing concern, which has become one of the most important research subjects in seismology and earthquake engineering. The change pattern of terrain mainly involves canyons and hills. In recent decades, a certain amount of literatures on effects of ground motion by canyons or hills have been reported, which provided references for anti-seismic and antidetonation engineering. The wave function method is one of the most commonly used methods in SH-wave scattering analyses, by means of which, Trifunac (1992) solved plane SH-wave scattering of semi-cylindrical canyon; Yuan and Liao (1996) addressed plane SH-wave scattering by arbitrary arc shaped hill; Liang *et al.* (2005) derived an analytical solution for scattering of plane P

wave by a semi-cylindrical hill; Zhang (2010) reported an analytical solution to the two-dimension stationary dynamic response of alluvial valley containing arbitrary number of circular-arc-shaped layers excited by incident Rayleigh waves; Liu *et al.* (2010) presented a theoretical study of multiple scattering of SH waves by two hills of different geometries (a triangle and a semicircle) on a solid half-space; the 2-D scattering and diffraction of plane SH waves induced by a non-symmetrical V-shaped canyon was examined (Zhang *et al.*, 2012); combined with the methods of complex function and moving coordinate system, Qi *et al.* (2012) provided the analytical solution to the problem of scattering of SH-wave induced by scalene triangular hill on a right-angle field; Lee *et al.* (2004), Lee and Alongkorn (2013) focused on the two-dimensional scattering of anti-plane (SH) waves by a semi-cylindrical hill with a semi-cylindrical concentric tunnel inside an elastic half-space, a shallow semi-elliptical hill on an elastic half-space; Chang *et al.* (2013) investigated the scattering of plane SH waves incident on a circular sectorial canyon. Since 1995, in application of complex variables, Liu and Han (1990), Liu and Liu (1997), Cui *et al.* (1998), Liu *et al.* (1998), Cao *et al.* (2001), Qiu and Liu (2005), Liu and Wang (2006), Lu and Liu (2006), Liu and Liu (2007), Liu *et al.* (2008), Li *et al.* (2008), Du *et al.* (2009), Lu *et al.* (2009), Liu *et al.* (2010) and Zhang (2010) successively derived a series of solution for elastic wave scattering by distinct terrain such as a cylindrical canyon, a cylindrical hill of circular-arc cross section, semi-cylindrical hills, a cylindrical hill of arbitrary shape, an isosceles triangular hill, isosceles triangular and semi-circular hills, multiple semi-cylindrical hills, a semi-cylindrical hill and canyon,

Correspondence to: Yang Zailin, College of Aerospace and Civil Engineering, Harbin Engineering University, Harbin 150001, China
Tel: +86 451 82519956; Fax: +86 451 82519210
E-mail: yangzailin00@163.com

[†]Professor; [‡]PhD Candidate

Supported by: Natural Science Foundation of Heilongjiang Province, China under Grant No. A201310, and the Scientific Research Starting Foundation for Post Doctorate of Heilongjiang Province, China under Grant No. LBH-Q13040

Received June 6, 2013; **Accepted** May 13, 2014

an isosceles triangular hill above a subsurface cavity, a semi-cylindrical hill with a hole and multiple cavities, a subsurface cavity with a nearby semi-cylindrical hill as well as canyons with variable depth-to-width ratio; Nazaret *et al.* (2003) analyzed antiplane deformations around arbitrary-shaped canyons on a wedge-shape half space. Additionally, some other important approaches have also been carried out by many contributions. A hybrid method which combines the finite element and series expansion method was implemented to solve the response of surface motion inside and near an irregular area embedded into an elastic half-plane (Shyu and Teng, 2011). The problem of SH-waves diffracted by a semi-circular hill was revisited using the null-field boundary integral equation method (BIEM) (Chen *et al.*, 2011). Tsaur and Hsu (2013) developed the region-point-matching technique (RPMT) to study the scattering of SH-waves disturbed by a partially filled semi-elliptic alluvial valley.

In railway engineering, multiple mountains and river valleys are common, which will bring a considerable amount of inconvenience. This type of terrain can be simplified as multiple triangular hills and canyons. However, few efforts were paid to this terrain owing to its complexity in boundary condition to date. The aim of the present paper is to investigate the scattering of two scalene triangular hills and a semi-cylindrical canyon by incident SH-waves based on “division” and “conjunction” technique which have been verified in Liu *et al.*'s work.

2 Analytical model

Given as Fig. 1 is a half-space model of two scalene triangular hills and a semi-cylindrical canyon under incident SH-waves, where the horizontal surface is denoted by S , the acmes of the hills by O and O_4 respectively, the triangle wedges' gradients as $1:n_1$, $1:n_2$, $1:n_3$ and $1:n_4$, the bottom margins as $2R_1$, the height of hills by h_1 and h_2 , the center of the semi-cylindrical canyon with boundary D_2 as O_2 and the

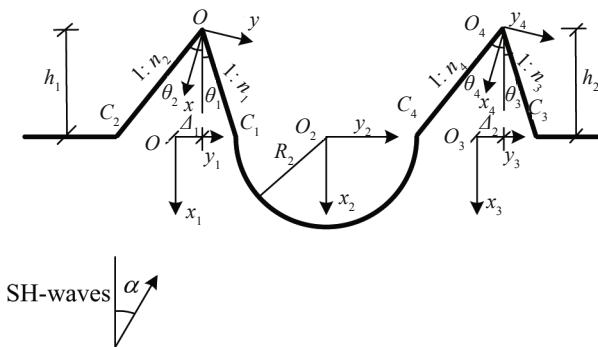


Fig. 1 Analytical model of two triangle hills and a semi-cylindrical canyon

associated radius as R_2 . To solve this problem, the model is divided into three parts as shown in Fig. 2. Domain I and II consist of scalene triangular hill and a semi-cylindrical bottom respectively and Domain III involves a half space with three semi-cylindrical canyons. Arc D_1 and D_3 stand for the interface between Domain I and II and Domain III and II, respectively, at which the stresses and displacements must be guaranteed to be continuous.

Supposing that the distance between O_1 and O_2 (O_3 and O_2) are d_1 , the distance between O_1 and O_3 are d_2 , and the projection of $|O_1O_2|$ and $|O_3O_4|$ on the bottom are Δ_1 and Δ_2 , and $R_1 = 1.0$, $R_2 = 0.5$, then

$$d_1 = R_1 + R_2, \quad d_2 = 2R_1 + 2R_2,$$

$$\Delta_1 = (n_2 - n_1)/(n_2 + n_1), \quad \Delta_2 = (n_4 - n_3)/(n_4 + n_3)$$

3 Governing equation

In an isotropic medium, the scattering of SH-waves is the simplest problem among the scattering problems of elastic waves. Introducing complex variables $z = x + iy$, $\bar{z} = x - iy$, the SH-wave Helmholtz expansion turns to be

$$\frac{\partial^2 W}{\partial z \partial \bar{z}} + \frac{1}{4} k^2 W = 0 \tag{1}$$

where $k = \omega/c_s$, in which ω represents the circular frequency of wave function, $c_s = \sqrt{\mu/\rho}$ is the propagation velocity of the shear wave, and ρ and μ are the mass density and shear modulus of the medium, respectively.

In polar coordinates system, the corresponding stresses are given by

$$\tau_{rz} = \mu \left(\frac{\partial W}{\partial z} e^{i\theta} + \frac{\partial W}{\partial \bar{z}} e^{-i\theta} \right), \tau_{\theta z} = i\mu \left(\frac{\partial W}{\partial z} e^{i\theta} - \frac{\partial W}{\partial \bar{z}} e^{-i\theta} \right) \tag{2}$$

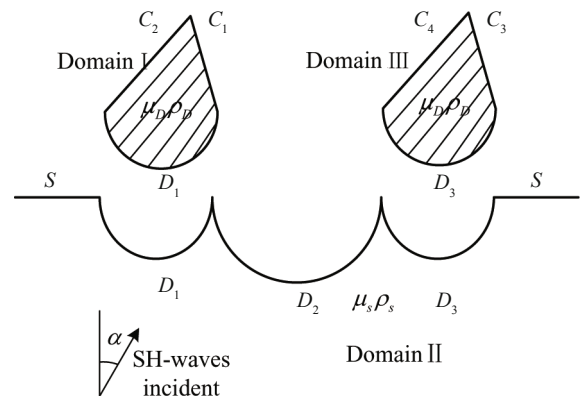


Fig. 2 The division of the solution domain

4 Problem statement

4.1 Standing waves in Domain I and III

In Domain I, the standing wave W^{D1} should obey the stress free condition on the wedge as

$$\tau_{\theta z}^{D1} = \begin{cases} 0, & \theta = +(\theta_1 + \theta_2)/2 \\ 0, & \theta = -(\theta_1 + \theta_2)/2 \end{cases} \quad (3)$$

In complex coordinates, the standing wave W^{D1} satisfying governing equation and boundary condition equation can be written as

$$W_1 = W^{D1}(Z, \bar{Z}) = W_0 \sum_{m=0}^{\infty} \left\{ D_m^{(1)} J_{2mp_1}(k_D |Z|) \left[\left(\frac{Z}{|Z|} \right)^{2mp_1} + \left(\frac{Z}{|Z|} \right)^{-2mp_1} \right] + D_m^{(2)} J_{(2m+1)p_1}(k_D |Z|) \left[\left(\frac{Z}{|Z|} \right)^{(2m+1)p_1} - \left(\frac{Z}{|Z|} \right)^{-(2m+1)p_1} \right] \right\} \quad (4)$$

where, W_0 denotes the displacement amplitude of standing wave, $D_m^{(1)}$ and $D_m^{(2)}$ are unknown coefficients, $p_1 = \pi/(\theta_1 + \theta_2)$, and $J_{2mp_1}(\cdot)$, $J_{(2m+1)p_1}(\cdot)$ are Bessel functions with $2mp_1$ and $(2m+1)p_1$ rank, respectively.

Depicted by Fig. 1, Z can be turned into

$$Z = (Z_1 + b_1)e^{iq_1} \quad (5)$$

wherein, $q_1 = (\arctan n_2 - \arctan n_1)/2$ and $b_1 = h_1 - \Delta_1 i$.

Consequently, in the complex plane (Z_1, \bar{Z}_1) , Eq. (4) transforms into

$$W^{D1}(Z_1, \bar{Z}_1) = W_0 \sum_{m=0}^{\infty} \left\{ D_m^{(1)} J_{2mp_1}(k_D |(Z_1 + b_1)e^{iq_1}|) \cdot \left[\left(\frac{(Z_1 + b_1)e^{iq_1}}{|(Z_1 + b_1)e^{iq_1}|} \right)^{2mp_1} + \left(\frac{(Z_1 + b_1)e^{iq_1}}{|(Z_1 + b_1)e^{iq_1}|} \right)^{-2mp_1} \right] + D_m^{(2)} J_{(2m+1)p_1}(k_D |(Z_1 + b_1)e^{iq_1}|) \cdot \left[\left(\frac{(Z_1 + b_1)e^{iq_1}}{|(Z_1 + b_1)e^{iq_1}|} \right)^{(2m+1)p_1} - \left(\frac{(Z_1 + b_1)e^{iq_1}}{|(Z_1 + b_1)e^{iq_1}|} \right)^{-(2m+1)p_1} \right] \right\} \quad (6)$$

Substitution of Eq. (4) into Eq. (2) yields the corresponding stress expression

$$\tau_{\eta z}^{D1}(Z_1, \bar{Z}_1) = \frac{\mu_D k_D W_0}{2} \sum_{m=0}^{\infty} \left\{ D_m^{(1)} P_{2mp_1}^{(D)}((Z_1 + b_1)e^{iq_1}) + D_m^{(2)} U_{(2m+1)p_1}^{(D)}((Z_1 + b_1)e^{iq_1}) \right\} \quad (7)$$

wherein,

$$P_t(s) = J_{t-1}(k|s|) \left[\frac{s}{|s|} \right]^{t-1} e^{i\theta} - J_{t+1}(k|s|) \left[\frac{s}{|s|} \right]^{-t-1} e^{i\theta} + J_{t-1}(k|s|) \left[\frac{s}{|s|} \right]^{1-t} e^{-i\theta} - J_{t+1}(k|s|) \left[\frac{s}{|s|} \right]^{-t+1} e^{-i\theta}$$

$$U_t(s) = J_{t-1}(k|s|) \left[\frac{s}{|s|} \right]^{t-1} e^{i\theta} + J_{t+1}(k|s|) \left[\frac{s}{|s|} \right]^{-t-1} e^{i\theta} - J_{t-1}(k|s|) \left[\frac{s}{|s|} \right]^{1-t} e^{-i\theta} - J_{t+1}(k|s|) \left[\frac{s}{|s|} \right]^{-t+1} e^{-i\theta}$$

Similarly to Domain I in derivation method, the standing wave of Domain III in the complex coordinate (Z_3, \bar{Z}_3) is swiftly deduced according to Eq. (6).

$$W^{D2}(Z_3, \bar{Z}_3) = W_0 \sum_{m=0}^{\infty} \left\{ E_m^{(1)} J_{2mp_2}(k_D |(Z_3 + b_2)e^{iq_2}|) \cdot \left[\left(\frac{(Z_3 + b_2)e^{iq_2}}{|(Z_3 + b_2)e^{iq_2}|} \right)^{2mp_2} + \left(\frac{(Z_3 + b_2)e^{iq_2}}{|(Z_3 + b_2)e^{iq_2}|} \right)^{-2mp_2} \right] + E_m^{(2)} J_{(2m+1)p_2}(k_D |(Z_3 + b_2)e^{iq_2}|) \cdot \left[\left(\frac{(Z_3 + b_2)e^{iq_2}}{|(Z_3 + b_2)e^{iq_2}|} \right)^{(2m+1)p_2} - \left(\frac{(Z_3 + b_2)e^{iq_2}}{|(Z_3 + b_2)e^{iq_2}|} \right)^{-(2m+1)p_2} \right] \right\} \quad (8)$$

wherein, $p_2 = \pi/(\theta_3 + \theta_4)$, $q_2 = (\arctan n_4 - \arctan n_3)/2$, $b_2 = h_2 - \Delta_2 i$, $E_m^{(1)}$ and $E_m^{(2)}$ are unknown coefficients. The associated stresses $\tau_{\eta z}^{D2}(Z_3, \bar{Z}_3)$ is obtained by substituting Eq. (8) into Eq. (2).

$$\tau_{\eta z}^{D2}(Z_3, \bar{Z}_3) = \frac{\mu_D k_D W_0}{2} \sum_{m=0}^{\infty} \left\{ E_m^{(1)} P_{2mp_2}^{(D)}((Z_3 + b_2)e^{iq_2}) + E_m^{(2)} U_{(2m+1)p_2}^{(D)}((Z_3 + b_2)e^{iq_2}) \right\} \quad (9)$$

4.2 Scattering waves in Domain II

Under incident SH-waves, the scattering waves in domain II generated by semi-cylindrical canyons (shown as Fig. 2), which should be free in stress on the horizontal surface, can be expressed in the complex planes (Z_i, \bar{Z}_i) ($i=1, 2, 3$) as follows

$$W^{S1}(Z_i, \bar{Z}_i) = W_0 \sum_{m=0}^{\infty} \left\{ A_m^{(1)} H_{2m}(k_S |\xi_{1i}|) \left[\left(\frac{\xi_{1i}}{|\xi_{1i}|} \right)^{2m} + \left(\frac{\xi_{1i}}{|\xi_{1i}|} \right)^{-2m} \right] + A_m^{(2)} H_{2m+1}(k_S |\xi_{1i}|) \left[\left(\frac{\xi_{1i}}{|\xi_{1i}|} \right)^{(2m+1)} - \left(\frac{\xi_{1i}}{|\xi_{1i}|} \right)^{-(2m+1)} \right] \right\}$$

$$(\xi_{1i} = Z_1, Z_2 + id_1, Z_3 + id_2; i=1, 2, 3) \quad (10)$$

$$W^{S2}(Z_i, \bar{Z}_i) = W_0 \sum_{m=0}^{\infty} \left\{ B_m^{(1)} H_{2m}(k_S |\xi_{2i}|) \left[\left(\frac{\xi_{2i}}{|\xi_{2i}|} \right)^{2m} + \left(\frac{\xi_{2i}}{|\xi_{2i}|} \right)^{-2m} \right] + B_m^{(2)} H_{2m+1}(k_S |\xi_{2i}|) \left[\left(\frac{\xi_{2i}}{|\xi_{2i}|} \right)^{(2m+1)} - \left(\frac{\xi_{2i}}{|\xi_{2i}|} \right)^{-(2m+1)} \right] \right\}$$

$$(\xi_{2i} = Z_1 - id_1, Z_2, Z_3 + id_1; i=1, 2, 3) \quad (11)$$

$$W^{S3}(Z_i, \bar{Z}_i) = W_0 \sum_{m=0}^{\infty} \left\{ C_m^{(1)} H_{2m}(k_S |\xi_{3i}|) \left[\left(\frac{\xi_{3i}}{|\xi_{3i}|} \right)^{2m} + \left(\frac{\xi_{3i}}{|\xi_{3i}|} \right)^{-2m} \right] + C_m^{(2)} H_{2m+1}(k_S |\xi_{3i}|) \left[\left(\frac{\xi_{3i}}{|\xi_{3i}|} \right)^{(2m+1)} - \left(\frac{\xi_{3i}}{|\xi_{3i}|} \right)^{-(2m+1)} \right] \right\}$$

$$(\xi_{3i} = Z_1 - id_2, Z_2 - id_1, Z_3; i=1, 2, 3) \quad (12)$$

Substituting above three expressions in Eq. (2), we have the expressions of the corresponding stresses as follows

$$\tau_{r_z}^{S1}(Z_i, \bar{Z}_i) = \frac{\mu_S k_S W_0}{2} \sum_{m=0}^{\infty} \left\{ A_m^{(1)} Q_{2m}^{S1}(\xi_{1i}) + A_m^{(2)} V_{2m+1}^{S1}(\xi_{1i}) \right\}$$

$$(\xi_{1i} = Z_1, Z_2 + id_1, Z_3 + id_2; i=1, 2, 3) \quad (13)$$

$$\tau_{r_z}^{S2}(Z_i, \bar{Z}_i) = \frac{\mu_S k_S W_0}{2} \sum_{m=0}^{\infty} \left\{ B_m^{(1)} Q_{2m}^{S2}(\xi_{2i}) + B_m^{(2)} V_{2m+1}^{S2}(\xi_{2i}) \right\}$$

$$(\xi_{2i} = Z_1 - id_1, Z_2, Z_3 + id_1; i=1, 2, 3) \quad (14)$$

$$\tau_{r_z}^{S3}(Z_i, \bar{Z}_i) = \frac{\mu_S k_S W_0}{2} \sum_{m=0}^{\infty} \left\{ C_m^{(1)} Q_{2m}^{S3}(\xi_{3i}) + C_m^{(2)} V_{2m+1}^{S3}(\xi_{3i}) \right\}$$

$$(\xi_{3i} = Z_1 - id_2, Z_2 - id_1, Z_3; i=1, 2, 3) \quad (15)$$

in which,

$$Q_t(s) = H_{t-1}^{(1)}(k_S |s|) \left[\frac{s}{|s|} \right]^{t-1} e^{i\theta} - H_{t+1}^{(1)}(k_S |s|) \left[\frac{s}{|s|} \right]^{t-1} e^{i\theta} + H_{t-1}^{(1)}(k_S |s|) \left[\frac{s}{|s|} \right]^{1-t} e^{-i\theta} - H_{t+1}^{(1)}(k_S |s|) \left[\frac{s}{|s|} \right]^{t+1} e^{-i\theta}$$

$$V_t(s) = H_{t-1}^{(1)}(k_S |s|) \left[\frac{s}{|s|} \right]^{t-1} e^{i\theta} + H_{t+1}^{(1)}(k_S |s|) \left[\frac{s}{|s|} \right]^{-t-1} e^{i\theta} - H_{t-1}^{(1)}(k_S |s|) \left[\frac{s}{|s|} \right]^{1-t} e^{-i\theta} - H_{t+1}^{(1)}(k_S |s|) \left[\frac{s}{|s|} \right]^{t+1} e^{-i\theta}$$

4.3 Incident wave and reflected wave

As shown in Fig. 1, SH-waves are incident into $X_1 Y_1 O_1$ coordinate system with an angle α , and subsequently, in complex coordinates (Z_i, \bar{Z}_i) , the incident wave and reflected wave can be written as

$$W^{i+r}(Z_i, \bar{Z}_i) = W_0 \left\{ 2J_0(k_S |\xi_{1i}|) + 2 \sum_{m=1}^{\infty} (-1)^m J_{2m}(k_S |\xi_{1i}|) \cos 2m\alpha - \left[\left(\frac{\xi_{1i}}{|\xi_{1i}|} \right)^{2m} + \left(\frac{\xi_{1i}}{|\xi_{1i}|} \right)^{-2m} \right] + 2 \sum_{m=0}^{\infty} (-1)^m J_{2m+1}(k_S |\xi_{1i}|) \sin(2m+1)\alpha - \left[\left(\frac{\xi_{1i}}{|\xi_{1i}|} \right)^{2m+1} - \left(\frac{\xi_{1i}}{|\xi_{1i}|} \right)^{-(2m+1)} \right] \right\}$$

$$(\xi_{1i} = Z_1, Z_2 + id_1, Z_3 + id_2; i=1, 2, 3) \quad (16)$$

Combined with Eq. (2), the related stresses $\tau_{r_z}^{i+r}(Z_i, \bar{Z}_i)$ can be derived.

$$\tau_{r_z}^{i+r}(Z_i, \bar{Z}_i) = \frac{\mu_S k_S W_0}{2} \times 2 \times \frac{J_{-1}(k_S |\xi_{1i}|) - J_1(k_S |\xi_{1i}|)}{2} \left\{ \left[\frac{\xi_{1i}}{|\xi_{1i}|} \right]^{-1} e^{i\theta} + \left[\frac{\xi_{1i}}{|\xi_{1i}|} \right]^1 e^{-i\theta} \right\} + \frac{\mu_S k_S W_0}{2} \sum_{m=1}^{\infty} 2(-1)^m \cos 2m\alpha P_{2m}^{(S)}(\xi_{1i}) + \frac{\mu_S k_S W_0}{2} \sum_{m=0}^{\infty} 2(-1)^m \sin(2m+1)\alpha U_{2m+1}^{(S)}(\xi_{1i}) \quad (17)$$

5 Solutions

Based on the ‘‘conjunction’’ condition that demands continuous displacement and stress at the shared boundary of domain I and II (domain III and II), a series of definite equations for solving unknown coefficients $D_m^{(j)}$, $E_m^{(j)}$, $A_m^{(j)}$, $B_m^{(j)}$ and $C_m^{(j)}$ ($j=1, 2$) can be deduced in combination with zero-stress condition on boundary edge of the semi-cylindrical canyon

$$\begin{cases}
 W_{(Z_1, \bar{Z}_1)}^{D1} = W_{(Z_1, \bar{Z}_1)}^{S1} + W_{(Z_1, \bar{Z}_1)}^{S2} + W_{(Z_1, \bar{Z}_1)}^{S3} + W_{(Z_1, \bar{Z}_1)}^{i+r} & Z_1 \in D_1 \\
 \tau_{\eta_1 z_1}^{D1} = \tau_{\eta_1 z_1}^{S1} + \tau_{\eta_1 z_1}^{S2} + \tau_{\eta_1 z_1}^{S3} + \tau_{\eta_1 z_1}^{i+r} & Z_1 \in D_1 \\
 W_{(Z_3, \bar{Z}_3)}^{D2} = W_{(Z_3, \bar{Z}_3)}^{S1} + W_{(Z_3, \bar{Z}_3)}^{S2} + W_{(Z_3, \bar{Z}_3)}^{S3} + W_{(Z_3, \bar{Z}_3)}^{i+r} & Z_3 \in D_3 \\
 \tau_{r_3 z_3}^{D1} = \tau_{r_3 z_3}^{S1} + \tau_{r_3 z_3}^{S2} + \tau_{r_3 z_3}^{S3} + \tau_{r_3 z_3}^{i+r} & Z_3 \in D_3 \\
 \tau_{r_2 z_2}^{S1} + \tau_{r_2 z_2}^{S2} + \tau_{r_2 z_2}^{S3} + \tau_{r_2 z_2}^{i+r} = 0 & Z_2 \in D_2
 \end{cases} \quad (18)$$

After insertion of the corresponding displacement and stress expressions, above equations can be transformed into Fourier series

$$\begin{cases}
 \sum_{n=0}^{\infty} \sum_{m=0}^{\infty} \psi_{mn}^{(1)} D_m^{(1)} - \sum_{n=0}^{\infty} \sum_{m=0}^{\infty} \eta_{mn}^{(1)} A_m^{(1)} - \sum_{n=0}^{\infty} \sum_{m=0}^{\infty} \phi_{mn}^{(1)} B_m^{(1)} - \sum_{n=0}^{\infty} \sum_{m=0}^{\infty} \varphi_{mn}^{(1)} C_m^{(1)} = \sum_{n=0}^{\infty} \sum_{m=0}^{\infty} \beta_{mn}^{(1)} \\
 \frac{\mu_D k_D}{\mu_S k_S} \sum_{n=0}^{\infty} \sum_{m=0}^{\infty} \psi_{mn}^{(11)} D_m^{(1)} - \sum_{n=0}^{\infty} \sum_{m=0}^{\infty} \eta_{mn}^{(11)} A_m^{(1)} - \sum_{n=0}^{\infty} \sum_{m=0}^{\infty} \phi_{mn}^{(11)} B_m^{(1)} - \sum_{n=0}^{\infty} \sum_{m=0}^{\infty} \varphi_{mn}^{(11)} C_m^{(1)} = \sum_{n=0}^{\infty} \sum_{m=0}^{\infty} \beta_{mn}^{(11)} \\
 \sum_{n=0}^{\infty} \sum_{m=0}^{\infty} \psi_{mn}^{(3)} E_m^{(1)} - \sum_{n=0}^{\infty} \sum_{m=0}^{\infty} \eta_{mn}^{(3)} A_m^{(1)} - \sum_{n=0}^{\infty} \sum_{m=0}^{\infty} \phi_{mn}^{(3)} B_m^{(1)} - \sum_{n=0}^{\infty} \sum_{m=0}^{\infty} \varphi_{mn}^{(3)} C_m^{(1)} = \sum_{n=0}^{\infty} \sum_{m=0}^{\infty} \beta_{mn}^{(3)} \\
 \frac{\mu_D k_D}{\mu_S k_S} \sum_{n=0}^{\infty} \sum_{m=0}^{\infty} \psi_{mn}^{(31)} E_m^{(1)} - \sum_{n=0}^{\infty} \sum_{m=0}^{\infty} \eta_{mn}^{(31)} A_m^{(1)} - \sum_{n=0}^{\infty} \sum_{m=0}^{\infty} \phi_{mn}^{(31)} B_m^{(1)} - \sum_{n=0}^{\infty} \sum_{m=0}^{\infty} \varphi_{mn}^{(31)} C_m^{(1)} = \sum_{n=0}^{\infty} \sum_{m=0}^{\infty} \beta_{mn}^{(31)} \\
 \sum_{n=0}^{\infty} \sum_{m=0}^{\infty} \eta_{mn}^{(51)} A_m^{(1)} + \sum_{n=0}^{\infty} \sum_{m=0}^{\infty} \phi_{mn}^{(51)} B_m^{(1)} + \sum_{n=0}^{\infty} \sum_{m=0}^{\infty} \varphi_{mn}^{(51)} C_m^{(1)} = \sum_{n=0}^{\infty} \sum_{m=0}^{\infty} \beta_{mn}^{(51)}
 \end{cases} \quad (19)$$

$$\begin{cases}
 \sum_{n=0}^{\infty} \sum_{m=0}^{\infty} \psi_{mn}^{(2)} D_m^{(2)} - \sum_{n=0}^{\infty} \sum_{m=0}^{\infty} \eta_{mn}^{(2)} A_m^{(2)} - \sum_{n=0}^{\infty} \sum_{m=0}^{\infty} \phi_{mn}^{(2)} B_m^{(2)} - \sum_{n=0}^{\infty} \sum_{m=0}^{\infty} \varphi_{mn}^{(2)} C_m^{(2)} = \sum_{n=0}^{\infty} \sum_{m=0}^{\infty} \beta_{mn}^{(2)} \\
 \frac{\mu_D k_D}{\mu_S k_S} \sum_{n=0}^{\infty} \sum_{m=0}^{\infty} \psi_{mn}^{(21)} D_m^{(2)} - \sum_{n=0}^{\infty} \sum_{m=0}^{\infty} \eta_{mn}^{(21)} A_m^{(2)} - \sum_{n=0}^{\infty} \sum_{m=0}^{\infty} \phi_{mn}^{(21)} B_m^{(2)} - \sum_{n=0}^{\infty} \sum_{m=0}^{\infty} \varphi_{mn}^{(21)} C_m^{(2)} = \sum_{n=0}^{\infty} \sum_{m=0}^{\infty} \beta_{mn}^{(21)} \\
 \sum_{n=0}^{\infty} \sum_{m=0}^{\infty} \psi_{mn}^{(4)} E_m^{(2)} - \sum_{n=0}^{\infty} \sum_{m=0}^{\infty} \eta_{mn}^{(4)} A_m^{(2)} - \sum_{n=0}^{\infty} \sum_{m=0}^{\infty} \phi_{mn}^{(4)} B_m^{(2)} - \sum_{n=0}^{\infty} \sum_{m=0}^{\infty} \varphi_{mn}^{(4)} C_m^{(2)} = \sum_{n=0}^{\infty} \sum_{m=0}^{\infty} \beta_{mn}^{(4)} \\
 \frac{\mu_D k_D}{\mu_S k_S} \sum_{n=0}^{\infty} \sum_{m=0}^{\infty} \psi_{mn}^{(41)} E_m^{(2)} - \sum_{n=0}^{\infty} \sum_{m=0}^{\infty} \eta_{mn}^{(41)} A_m^{(2)} - \sum_{n=0}^{\infty} \sum_{m=0}^{\infty} \phi_{mn}^{(41)} B_m^{(2)} - \sum_{n=0}^{\infty} \sum_{m=0}^{\infty} \varphi_{mn}^{(41)} C_m^{(2)} = \sum_{n=0}^{\infty} \sum_{m=0}^{\infty} \beta_{mn}^{(41)} \\
 \sum_{n=0}^{\infty} \sum_{m=0}^{\infty} \eta_{mn}^{(61)} A_m^{(2)} + \sum_{n=0}^{\infty} \sum_{m=0}^{\infty} \phi_{mn}^{(61)} B_m^{(2)} + \sum_{n=0}^{\infty} \sum_{m=0}^{\infty} \varphi_{mn}^{(61)} C_m^{(2)} = \sum_{n=0}^{\infty} \sum_{m=0}^{\infty} \beta_{mn}^{(61)}
 \end{cases} \quad (20)$$

where

$$\begin{aligned}
 \psi_{mn}^{(1)} &= \frac{1}{2\pi} \int_{-\frac{\pi}{2}}^{\frac{\pi}{2}} J_{2mp_1}(k_D |(Z_1 + b_1)e^{iq_1}|) \left\{ \left[\frac{(Z_1 + b_1)e^{iq_1}}{|(Z_1 + b_1)e^{iq_1}|} \right]^{2mp_1} + \left[\frac{(Z_1 + b_1)e^{iq_1}}{|(Z_1 + b_1)e^{iq_1}|} \right]^{-2mp_1} \right\} e^{-in\theta} d\theta \\
 \eta_{mn}^{(1)} &= \frac{1}{2\pi} \int_{-\frac{\pi}{2}}^{\frac{\pi}{2}} H_{2m}^{(1)}(k_S |Z_1|) \left\{ \left[\frac{Z_1}{|Z_1|} \right]^{2m} + \left[\frac{Z_1}{|Z_1|} \right]^{-2m} \right\} e^{-in\theta} d\theta \\
 \phi_{mn}^{(1)} &= \frac{1}{2\pi} \int_{-\frac{\pi}{2}}^{\frac{\pi}{2}} H_{2m}^{(1)}(k_S |Z_1 - id_1|) \left\{ \left[\frac{Z_1 - id_1}{|Z_1 - id_1|} \right]^{2m} + \left[\frac{Z_1 - id_1}{|Z_1 - id_1|} \right]^{-2m} \right\} e^{-in\theta} d\theta \\
 \varphi_{mn}^{(1)} &= \frac{1}{2\pi} \int_{-\frac{\pi}{2}}^{\frac{\pi}{2}} H_{2m}^{(1)}(k_S |Z_1 - id_2|) \left\{ \left[\frac{Z_1 - id_2}{|Z_1 - id_2|} \right]^{2m} + \left[\frac{Z_1 - id_2}{|Z_1 - id_2|} \right]^{-2m} \right\} e^{-in\theta} d\theta
 \end{aligned}$$

$$\beta_{mn}^{(1)} = \begin{cases} \frac{1}{2\pi} \int_{-\frac{\pi}{2}}^{\frac{\pi}{2}} 2J_0(k_S |Z_1|) e^{-in\theta} d\theta & m = 0 \\ \frac{1}{2\pi} \int_{-\frac{\pi}{2}}^{\frac{\pi}{2}} 2(-1)^m J_{2m}(k_S |Z_1|) \cos 2m\alpha \left\{ \left[\frac{Z_1}{|Z_1|} \right]^{2m} + \left[\frac{Z_1}{|Z_1|} \right]^{-2m} \right\} e^{-in\theta} d\theta & m > 0 \end{cases}$$

$$\psi_{mn}^{(11)} = \frac{1}{2\pi} \int_{-\frac{\pi}{2}}^{\frac{\pi}{2}} \{ P_{2mp_1}^{(D)}((Z_1 + b_1)e^{iq_1}) \} e^{-in\theta} d\theta \quad \eta_{mn}^{(11)} = \frac{1}{2\pi} \int_{-\frac{\pi}{2}}^{\frac{\pi}{2}} \{ Q_{2m}^{(S)}(Z_1) \} e^{-in\theta} d\theta$$

$$\phi_{mn}^{(11)} = \frac{1}{2\pi} \int_{-\frac{\pi}{2}}^{\frac{\pi}{2}} \{ Q_{2m}^{(S)}(Z_1 - id_1) \} e^{-in\theta} d\theta \quad \varphi_{mn}^{(11)} = \frac{1}{2\pi} \int_{-\frac{\pi}{2}}^{\frac{\pi}{2}} \{ Q_{2m}^{(S)}(Z_1 - id_2) \} e^{-in\theta} d\theta$$

$$\beta_{mn}^{(11)} = \begin{cases} \frac{1}{2\pi} \int_{-\frac{\pi}{2}}^{\frac{\pi}{2}} 2 \times \frac{J_{-1}(k_S |Z_1|) - J_1(k_S |Z_1|)}{2} \left\{ \left[\frac{Z_1}{|Z_1|} \right]^{-1} e^{i\theta} + \left[\frac{Z_1}{|Z_1|} \right]^1 e^{-i\theta} \right\} e^{-in\theta} d\theta & m = 0 \\ \frac{1}{2\pi} \int_{-\frac{\pi}{2}}^{\frac{\pi}{2}} 2(-1)^m \cos 2m\alpha P_{2m}^{(S)}(Z_1) e^{-in\theta} d\theta & m > 0 \end{cases}$$

$$\psi_{mn}^{(3)} = \frac{1}{2\pi} \int_{-\frac{\pi}{2}}^{\frac{\pi}{2}} J_{2mp_2}(k_D |(Z_3 + b_2)e^{iq_2}|) \left\{ \left[\frac{(Z_3 + b_2)e^{iq_2}}{|(Z_3 + b_2)e^{iq_2}|} \right]^{2mp_2} + \left[\frac{(Z_3 + b_2)e^{iq_2}}{|(Z_3 + b_2)e^{iq_2}|} \right]^{-2mp_2} \right\} e^{-in\theta} d\theta$$

$$\eta_{mn}^{(3)} = \frac{1}{2\pi} \int_{-\frac{\pi}{2}}^{\frac{\pi}{2}} H_{2m}^{(1)}(k_S |Z_3 + id_2|) \left\{ \left[\frac{Z_3 + id_2}{|Z_3 + id_2|} \right]^{2m} + \left[\frac{Z_3 + id_2}{|Z_3 + id_2|} \right]^{-2m} \right\} e^{-in\theta} d\theta$$

$$\phi_{mn}^{(3)} = \frac{1}{2\pi} \int_{-\frac{\pi}{2}}^{\frac{\pi}{2}} H_{2m}^{(1)}(k_S |Z_3 + id_1|) \left\{ \left[\frac{Z_3 + id_1}{|Z_3 + id_1|} \right]^{2m} + \left[\frac{Z_3 + id_1}{|Z_3 + id_1|} \right]^{-2m} \right\} e^{-in\theta} d\theta$$

$$\varphi_{mn}^{(3)} = \frac{1}{2\pi} \int_{-\frac{\pi}{2}}^{\frac{\pi}{2}} H_{2m}^{(1)}(k_S |Z_3|) \left\{ \left[\frac{Z_3}{|Z_3|} \right]^{2m} + \left[\frac{Z_3}{|Z_3|} \right]^{-2m} \right\} e^{-in\theta} d\theta$$

$$\beta_{mn}^{(3)} = \begin{cases} \frac{1}{2\pi} \int_{-\frac{\pi}{2}}^{\frac{\pi}{2}} 2J_0(k_S |Z_3 + id_2|) e^{-in\theta} d\theta & m = 0 \\ \frac{1}{2\pi} \int_{-\frac{\pi}{2}}^{\frac{\pi}{2}} 2(-1)^m J_{2m}(k_S |Z_3 + id_2|) \cos 2m\alpha \left\{ \left[\frac{Z_3 + id_2}{|Z_3 + id_2|} \right]^{2m} + \left[\frac{Z_3 + id_2}{|Z_3 + id_2|} \right]^{-2m} \right\} e^{-in\theta} d\theta & m > 0 \end{cases}$$

$$\psi_{mn}^{(31)} = \frac{1}{2\pi} \int_{-\frac{\pi}{2}}^{\frac{\pi}{2}} \{ P_{2mp_2}^{(D)}(Z_3 + id_2) \} e^{-in\theta} d\theta \quad \eta_{mn}^{(31)} = \frac{1}{2\pi} \int_{-\frac{\pi}{2}}^{\frac{\pi}{2}} \{ Q_{2m}^{(S)}(Z_3 + id_2) \} e^{-in\theta} d\theta$$

$$\phi_{mn}^{(31)} = \frac{1}{2\pi} \int_{-\frac{\pi}{2}}^{\frac{\pi}{2}} \{ Q_{2m}^{(S)}(Z_3 + id_1) \} e^{-in\theta} d\theta \quad \varphi_{mn}^{(31)} = \frac{1}{2\pi} \int_{-\frac{\pi}{2}}^{\frac{\pi}{2}} \{ Q_{2m}^{(S)}(Z_3) \} e^{-in\theta} d\theta$$

$$\beta_{mn}^{(31)} = \begin{cases} \frac{1}{2\pi} \int_{-\frac{\pi}{2}}^{\frac{\pi}{2}} 2 \times \frac{J_{-1}(k_S |Z_3 + id_2|) - J_1(k_S |Z_3 + id_2|)}{2} \left\{ \left[\frac{Z_3 + id_2}{|Z_3 + id_2|} \right]^{-1} e^{i\theta} + \left[\frac{Z_3 + id_2}{|Z_3 + id_2|} \right]^1 e^{-i\theta} \right\} e^{-in\theta} d\theta & m = 0 \\ \frac{1}{2\pi} \int_{-\frac{\pi}{2}}^{\frac{\pi}{2}} 2(-1)^m \cos 2m\alpha P_{2m}^{(S)} \left(\frac{Z_3 + id_2}{|Z_3 + id_2|} \right) e^{-in\theta} d\theta & m > 0 \end{cases}$$

$$\eta_{mn}^{(51)} = \frac{1}{2\pi} \int_{-\frac{\pi}{2}}^{\frac{\pi}{2}} \left\{ Q_{2m}^{(S)}(Z_2 + id_1) \right\} e^{-in\theta} d\theta \quad \phi_{mn}^{(51)} = \frac{1}{2\pi} \int_{-\frac{\pi}{2}}^{\frac{\pi}{2}} \left\{ Q_{2m}^{(S)}(Z_2) \right\} e^{-in\theta} d\theta$$

$$\varphi_{mn}^{(51)} = \frac{1}{2\pi} \int_{-\frac{\pi}{2}}^{\frac{\pi}{2}} \left\{ Q_{2m}^{(S)}(Z_2 - id_1) \right\} e^{-in\theta} d\theta$$

$$\beta_{mn}^{(51)} = \begin{cases} \frac{1}{2\pi} \int_{-\frac{\pi}{2}}^{\frac{\pi}{2}} 2 \times \frac{J_{-1}(k_S |Z_2 + id_1|) - J_1(k_S |Z_2 + id_1|)}{2} \left\{ \left[\frac{Z_2 + id_1}{|Z_2 + id_1|} \right]^{-1} e^{i\theta} + \left[\frac{Z_2 + id_1}{|Z_2 + id_1|} \right]^1 e^{-i\theta} \right\} e^{-in\theta} d\theta & m = 0 \\ \frac{1}{2\pi} \int_{-\frac{\pi}{2}}^{\frac{\pi}{2}} 2(-1)^m \cos 2m\alpha P_{2m}^{(S)}(Z_2 + id_1) e^{-in\theta} d\theta & m > 0 \end{cases}$$

$$\psi_{mn}^{(2)} = \frac{1}{2\pi} \int_{-\frac{\pi}{2}}^{\frac{\pi}{2}} J_{(2m+1)p_1}(k_D |(Z_1 + b_1)e^{iq_1}|) \left\{ \left[\frac{(Z_1 + b_1)e^{iq_1}}{|(Z_1 + b_1)e^{iq_1}|} \right]^{(2m+1)p_1} - \left[\frac{(Z_1 + b_1)e^{iq_1}}{|(Z_1 + b_1)e^{iq_1}|} \right]^{-(2m+1)p_1} \right\} e^{-in\theta} d\theta$$

$$\eta_{mn}^{(2)} = \frac{1}{2\pi} \int_{-\frac{\pi}{2}}^{\frac{\pi}{2}} H_{2m+1}^{(1)}(k_S |Z_1|) \left\{ \left[\frac{Z_1}{|Z_1|} \right]^{2m+1} - \left[\frac{Z_1}{|Z_1|} \right]^{-(2m+1)} \right\} e^{-in\theta} d\theta$$

$$\phi_{mn}^{(2)} = \frac{1}{2\pi} \int_{-\frac{\pi}{2}}^{\frac{\pi}{2}} H_{2m+1}^{(1)}(k_S |Z_1 - id_1|) \left\{ \left[\frac{Z_1 - id_1}{|Z_1 - id_1|} \right]^{2m+1} - \left[\frac{Z_1 - id_1}{|Z_1 - id_1|} \right]^{-(2m+1)} \right\} e^{-in\theta} d\theta$$

$$\varphi_{mn}^{(2)} = \frac{1}{2\pi} \int_{-\frac{\pi}{2}}^{\frac{\pi}{2}} H_{2m+1}^{(1)}(k_S |Z_1 - id_2|) \left\{ \left[\frac{Z_1 - id_2}{|Z_1 - id_2|} \right]^{2m+1} - \left[\frac{Z_1 - id_2}{|Z_1 - id_2|} \right]^{-(2m+1)} \right\} e^{-in\theta} d\theta$$

$$\beta_{mn}^{(2)} = \frac{1}{2\pi} \int_{-\frac{\pi}{2}}^{\frac{\pi}{2}} 2(-1)^m J_{2m+1}(k_S |Z_1|) \sin(2m+1)\alpha \left\{ \left[\frac{Z_1}{|Z_1|} \right]^{2m+1} - \left[\frac{Z_1}{|Z_1|} \right]^{-2m-1} \right\} e^{-in\theta} d\theta$$

$$\psi_{mn}^{(21)} = \frac{1}{2\pi} \int_{-\frac{\pi}{2}}^{\frac{\pi}{2}} \left\{ U_{(2m+1)p_1}^{(D)}((Z_1 + b_1)e^{iq_1}) \right\} e^{-in\theta} d\theta \quad \eta_{mn}^{(21)} = \frac{1}{2\pi} \int_{-\frac{\pi}{2}}^{\frac{\pi}{2}} \left\{ V_{2m+1}^{(S)}(Z_1) \right\} e^{-in\theta} d\theta$$

$$\phi_{mn}^{(21)} = \frac{1}{2\pi} \int_{-\frac{\pi}{2}}^{\frac{\pi}{2}} \left\{ V_{2m+1}^{(S)}(Z_1 - id_1) \right\} e^{-in\theta} d\theta \quad \varphi_{mn}^{(21)} = \frac{1}{2\pi} \int_{-\frac{\pi}{2}}^{\frac{\pi}{2}} \left\{ V_{2m+1}^{(S)}(Z_1 - id_2) \right\} e^{-in\theta} d\theta$$

$$\beta_{mn}^{(21)} = \frac{1}{2\pi} \int_{-\frac{\pi}{2}}^{\frac{\pi}{2}} 2(-1)^m \sin(2m+1)\alpha \left\{ U_{2m+1}^{(S)}(Z_1) \right\} e^{-in\theta} d\theta$$

$$\psi_{mn}^{(4)} = \frac{1}{2\pi} \int_{-\frac{\pi}{2}}^{\frac{\pi}{2}} J_{(2m+1)p_2}(k_D |(Z_3 + b_2)e^{iq_2}|) \left\{ \left[\frac{(Z_3 + b_2)e^{iq_2}}{|(Z_3 + b_2)e^{iq_2}|} \right]^{(2m+1)p_2} - \left[\frac{(Z_3 + b_2)e^{iq_2}}{|(Z_3 + b_2)e^{iq_2}|} \right]^{-(2m+1)p_2} \right\} e^{-in\theta} d\theta$$

$$\eta_{mn}^{(4)} = \frac{1}{2\pi} \int_{-\frac{\pi}{2}}^{\frac{\pi}{2}} H_{2m+1}^{(1)}(k_S |Z_3 + id_2|) \left\{ \left[\frac{Z_3 + id_2}{|Z_3 + id_2|} \right]^{2m+1} - \left[\frac{Z_3 + id_2}{|Z_3 + id_2|} \right]^{-(2m+1)} \right\} e^{-in\theta} d\theta$$

$$\phi_{mn}^{(4)} = \frac{1}{2\pi} \int_{-\frac{\pi}{2}}^{\frac{\pi}{2}} H_{2m+1}^{(1)}(k_S |Z_3 + id_1|) \left\{ \left[\frac{Z_3 + id_1}{|Z_3 + id_1|} \right]^{2m+1} - \left[\frac{Z_3 + id_1}{|Z_3 + id_1|} \right]^{-(2m+1)} \right\} e^{-in\theta} d\theta$$

$$\varphi_{mn}^{(4)} = \frac{1}{2\pi} \int_{-\frac{\pi}{2}}^{\frac{\pi}{2}} H_{2m+1}^{(1)}(k_S |Z_3|) \left\{ \left[\frac{Z_3}{|Z_3|} \right]^{2m+1} - \left[\frac{Z_3}{|Z_3|} \right]^{-(2m+1)} \right\} e^{-in\theta} d\theta$$

$$\beta_{mn}^{(4)} = \frac{1}{2\pi} \int_{-\frac{\pi}{2}}^{\frac{\pi}{2}} 2(-1)^m J_{2m+1}(k_s |Z_3 + id_2|) \sin(2m+1)\alpha \left\{ \left[\frac{Z_3 + id_2}{|Z_3 + id_2|} \right]^{2m+1} - \left[\frac{Z_3 + id_2}{|Z_3 + id_2|} \right]^{-2m-1} \right\} e^{-in\theta} d\theta$$

$$\psi_{mn}^{(41)} = \frac{1}{2\pi} \int_{-\frac{\pi}{2}}^{\frac{\pi}{2}} \left\{ U_{(2m+1)\rho_2}^{(D)}((Z_3 + b_2)e^{iq_2}) \right\} e^{-in\theta} d\theta \quad \eta_{mn}^{(41)} = \frac{1}{2\pi} \int_{-\frac{\pi}{2}}^{\frac{\pi}{2}} \left\{ V_{2m+1}^{(S)}(Z_3 + id_2) \right\} e^{-in\theta} d\theta$$

$$\phi_{mn}^{(41)} = \frac{1}{2\pi} \int_{-\frac{\pi}{2}}^{\frac{\pi}{2}} \left\{ V_{2m+1}^{(S)}(Z_3 + id_1) \right\} e^{-in\theta} d\theta \quad \varphi_{mn}^{(41)} = \frac{1}{2\pi} \int_{-\frac{\pi}{2}}^{\frac{\pi}{2}} \left\{ V_{2m+1}^{(S)}(Z_3) \right\} e^{-in\theta} d\theta$$

$$\beta_{mn}^{(41)} = \frac{1}{2\pi} \int_{-\frac{\pi}{2}}^{\frac{\pi}{2}} 2(-1)^m \sin(2m+1)\alpha \left\{ U_{2m+1}^{(S)}(Z_3 + id_2) \right\} e^{-in\theta} d\theta$$

$$\eta_{mn}^{(61)} = \frac{1}{2\pi} \int_{-\frac{\pi}{2}}^{\frac{\pi}{2}} \left\{ V_{2m+1}^{(S)}(Z_2 + id_1) \right\} e^{-in\theta} d\theta$$

$$\phi_{mn}^{(61)} = \frac{1}{2\pi} \int_{-\frac{\pi}{2}}^{\frac{\pi}{2}} \left\{ V_{2m+1}^{(S)}(Z_2) \right\} e^{-in\theta} d\theta \quad \varphi_{mn}^{(61)} = \frac{1}{2\pi} \int_{-\frac{\pi}{2}}^{\frac{\pi}{2}} \left\{ V_{2m+1}^{(S)}(Z_2 - id_1) \right\} e^{-in\theta} d\theta$$

$$\beta_{mn}^{(61)} = -\frac{1}{2\pi} \int_{-\frac{\pi}{2}}^{\frac{\pi}{2}} 2(-1)^m \sin(2m+1)\alpha \left\{ U_{2m+1}^{(S)}(Z_2 + id_1) \right\} e^{-in\theta} d\theta$$

Equations (19) and (20) were solved by utilizing the limitation truncation to satisfy the computation precision.

6 Displacement amplitudes

In Domain I and III, the total wave fields involve the standing waves W^{D1} and W^{D2} , respectively

$$W_I = W^{D1}, W_{III} = W^{D2} \tag{21}$$

In Domain II, the total wave field includes four displacement fields

$$W_{II} = W^{i+r} + W^{S1} + W^{S2} + W^{S3} \tag{22}$$

Equations (21) and (22) can be also expressed as

$$W_j = |W_j| e^{i(\omega t - \phi_j)} \quad j = I, II, III \tag{23}$$

where, $|W_j|$ is the displacement amplitude and ϕ_j the phase angle of W_j

$$\phi_j = \arctan \left[\frac{\text{Im} W_j}{\text{Re} W_j} \right] \tag{24}$$

7 Numerical results and discussions

As a numerical example, suppose that the districts are identical in material properties ($\rho_D = \rho_S, \mu_D = \mu_S, k_D = k_S$) and two scalene triangular hills in shape and height ($n_1 = n_3, n_2 = n_4, h_1 = h_2, \Delta_1 = \Delta_2$), and the

amplitude of incident wave $W_0 = 1.0$. For convenience, $y_1/R_1 \leq -1.0$ is defined as the horizontal surface at the left hand side and $4 \leq y_1/R_1 \leq 5$ at the right hand side. Hence, $|y_1/R_1| < 1.0$ indicates the first hill, $1 \leq y_1/R_1 < 2$ the canyon, $2 \leq y_1/R_1 < 4$ the second hill and $y_1/R_1 = \Delta_1$ the vertex of the first triangular hill. Besides, the vertex angles of triangular hill are defined as θ_0 . Based on above theoretical derivation, antiplane response of two scalene triangular hills and a semi-cylindrical canyon to incident SH-waves is investigated. The expressions of surface displacements $|W|$ are defined respectively by Eqs. (21) and (22).

In order to verify the computation precision of boundary condition and the analytical method used in this paper, the model is degenerated into one isosceles hill and the calculated results for hills with $\theta_0 = 60^\circ, 90^\circ$ and 120° under vertically incident SH-wave when $\eta = 0.5$ are given in Fig. 3. By comparing with the results for the same numerical example obtained by Qiu and Liu (2005), the results shown in Fig. 3 can be demonstrated to be accurate.

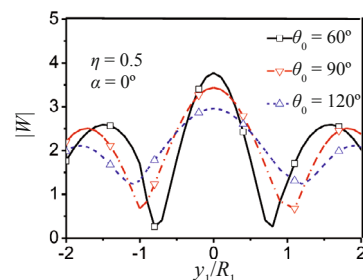


Fig. 3 Variation of surface displacements $|W|$ with y_1/R_1 when $\eta = 5$

Figures 4 to 8 are plotted to discuss the distribution of the surface displacement amplitudes influenced by different frequency η and incident angles in the case of $\theta_{21} = \theta_2 - \theta_1 = 0^\circ, 10^\circ, 20^\circ$. The vertex angles of triangular hills are assumed to be 138.2° under incident SH-waves in $X_1O_1Y_1$ coordinate system.

Figure 4 intuitively shows that, for $\eta = 0.1$, the surface displacement amplitudes $|W|$ change slightly whatever the incident angle α and θ_{21} vary, which denotes the quasi-static characteristic case, and the maximum amplitude $|W|_{\max} \approx 2.05$. From Figs. 5 to 8, it can be demonstrated that the dynamic characteristics of ground motion becomes more and more distinct and the surge of $|W|$ appears more and more evidently as well when η varies from 0.25 to 1.0.

The strong dependence of the surface displacement amplitudes $|W|$ on incident angle α can be revealed in Fig. 5 through Fig. 8. With the increase of α , surface displacement amplitudes $|W|$ of horizontal surface at the left hand side increase and those of the canyon, the second hill and the horizontal surface at the right-hand side decrease. It is just because SH-waves are incident into $X_1O_1Y_1$ coordinate system. The maximum displacement amplitude $|W|_{\max}$ always occurs at $y_1/R_1 = \Delta_1$ (the vertex of the first triangular hill) when SH-waves incident vertically described in Fig. 5(a),

Fig. 6(a), Fig. 7(a) and Fig. 8(a). For $\eta = 1.0$, $|W|_{\max} = 2.28, 2.52$ and 2.94 respectively when $\theta_{21} = 0^\circ, 10^\circ$, and 20° .

Figure 8 illustrates that, in the range of $1 \leq y_1/R_1 < 2$, a valley value of surface displacements of the canyon always occurs at $y_1/R_1 \approx 1.5$ and is getting larger with the increment of incident angle α when $\eta = 1.0$. Additionally, it can be also found that variation of θ_{21} impacts slightly on distribution of the surface displacement while the vertex angles of triangular hills are fixed. Compared with other cases, the whole surface displacement amplitudes $|W|$ seem to be far smaller when $\eta = 1.0$, as observed in Fig. 8.

3D graphs are provided in Fig. 9 to show the displacement amplitudes $|W|$ versus y_1/R_1 and vertex angle of the triangular hills θ_0 when frequency $\eta = 1.0$. Dynamic response of ground motion of the canyon, the second hill and the right horizontal surface depends strongly on vertex angle of the triangular hills θ_0 , as shown in Fig. 9. Taking Fig. 9(c) for example, the results show that the stronger is dynamic characteristics, the greater become the displacement amplitudes when the vertex angle varies between 60° and 90° (120° and 150°). Moreover, a valley value $|W| = 0.32$ appears at $y_1/R_1 \approx 3.0$ when $\theta_0 = 100^\circ$.

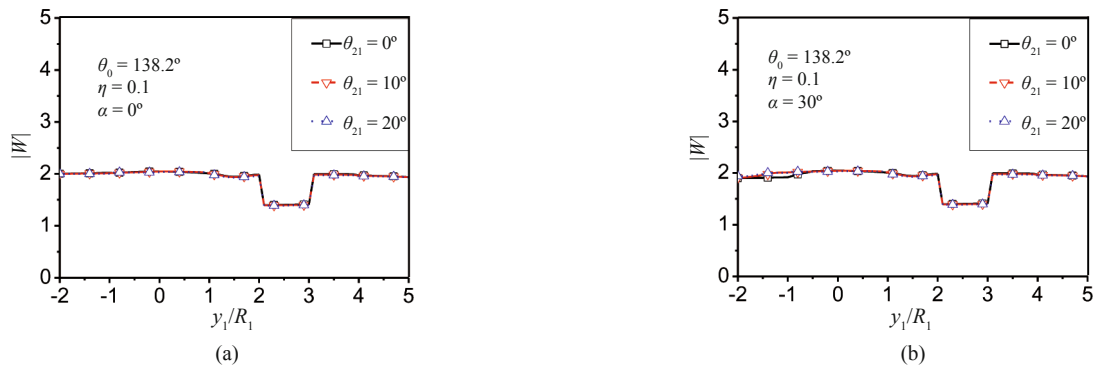


Fig. 4 Variation of surface displacements $|W|$ with y_1/R_1 when $\eta = 0.1$

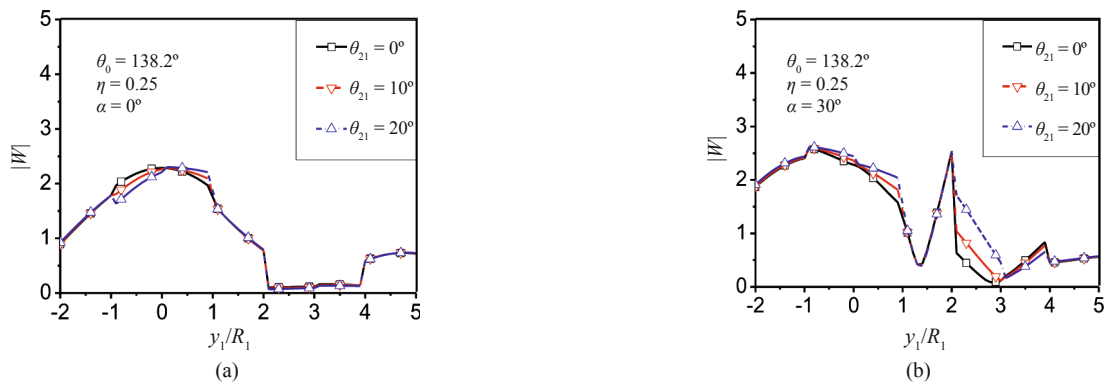


Fig. 5 Variation of surface displacements $|W|$ with y_1/R_1 when $\eta = 0.25$

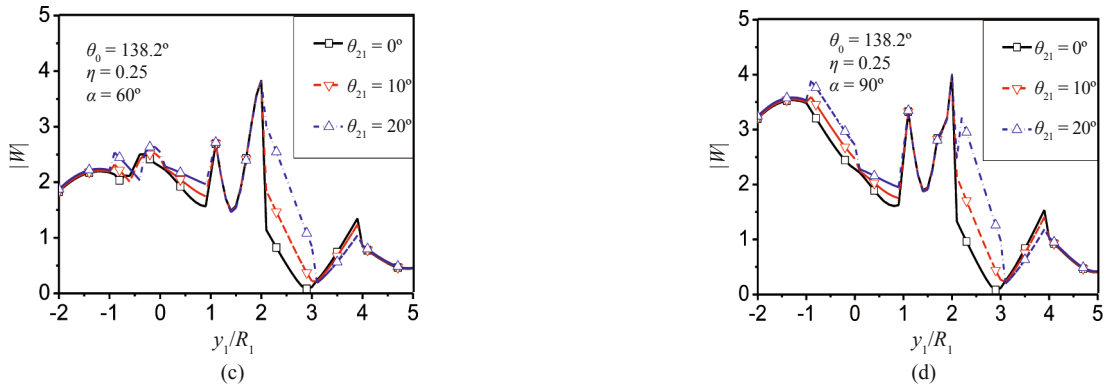


Fig. 5 Continued

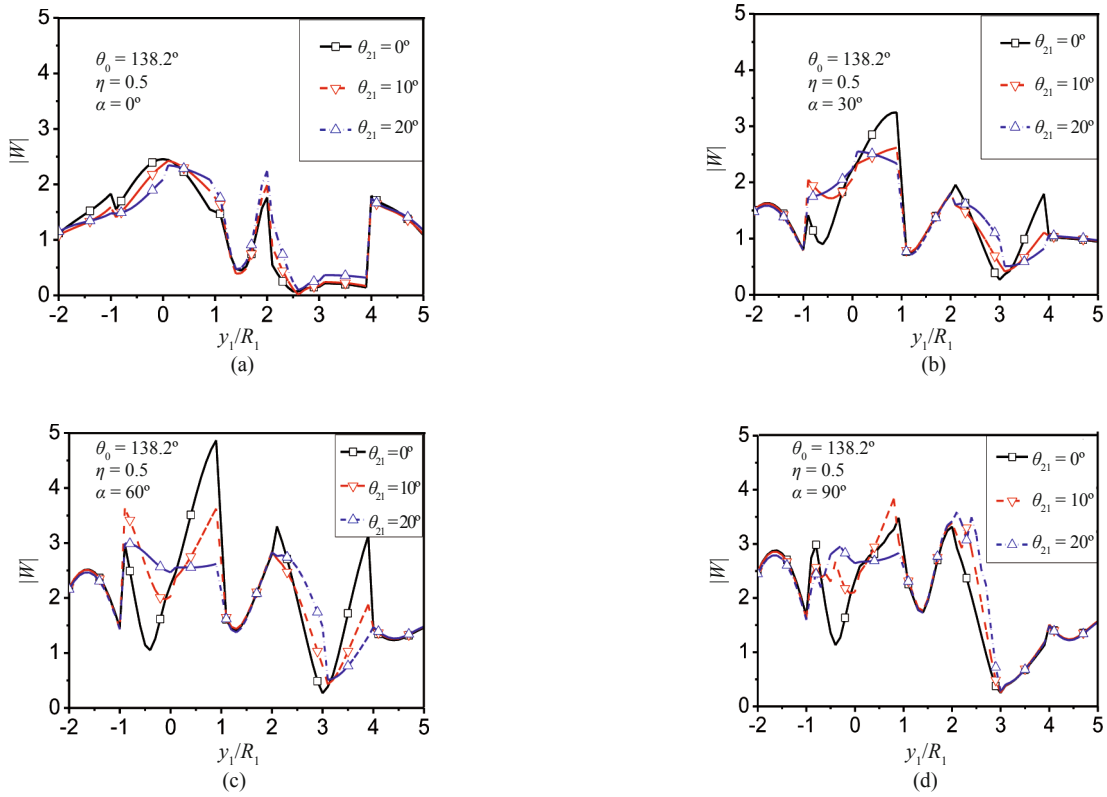


Fig. 6 Variation of surface displacements $|W|$ with y_1/R_1 when $\eta = 0.5$

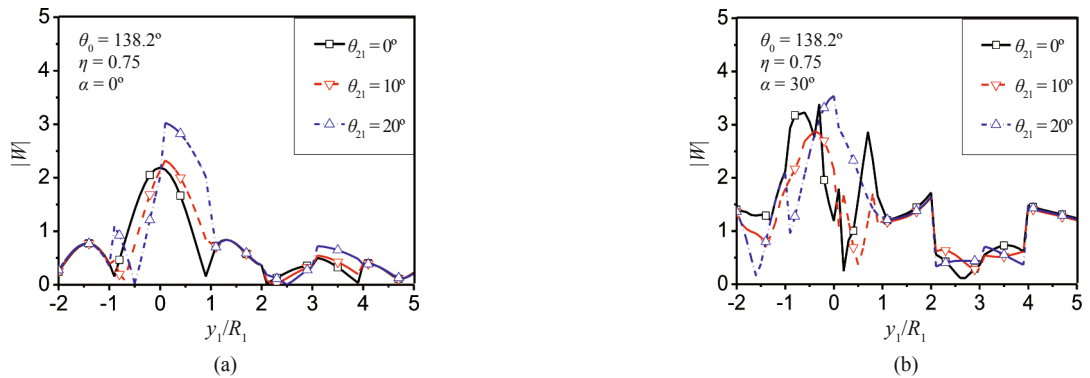


Fig. 7 Variation of surface displacements $|W|$ with y_1/R_1 when $\eta = 0.75$

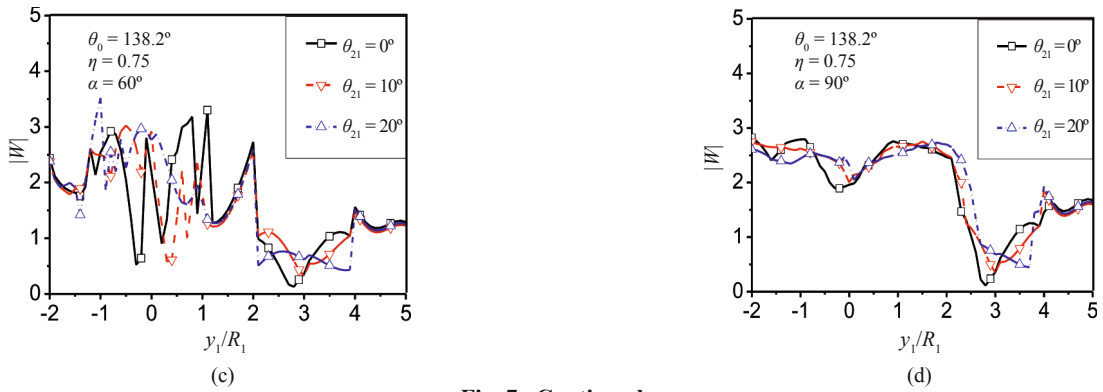


Fig. 7 Continued

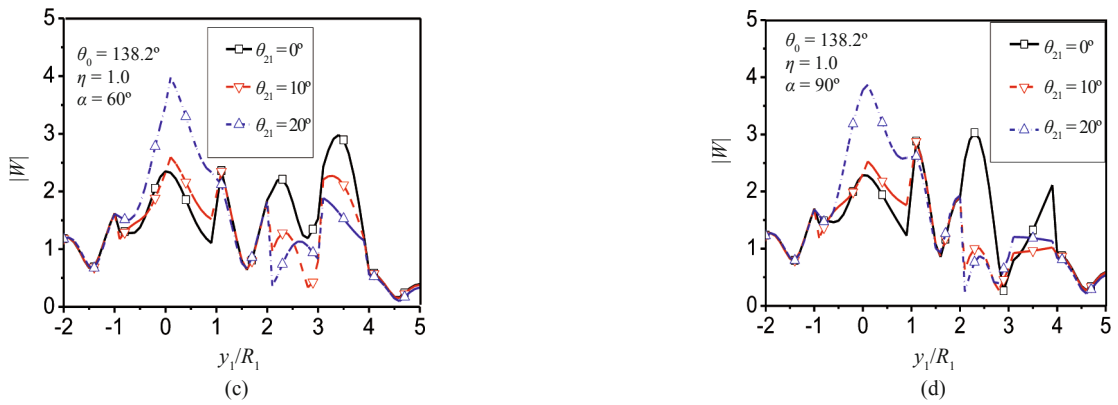
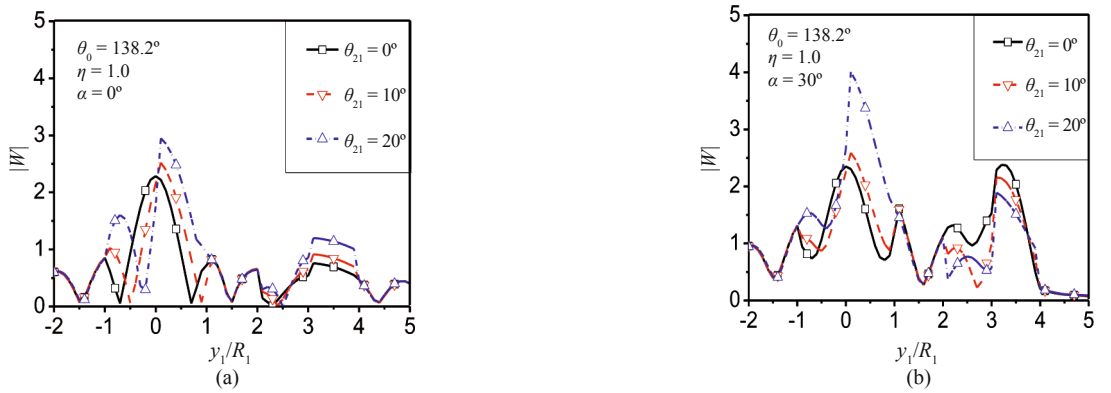


Fig. 8 Variation of surface displacements $|W|$ with y_1/R_1 when $\eta = 1.00$

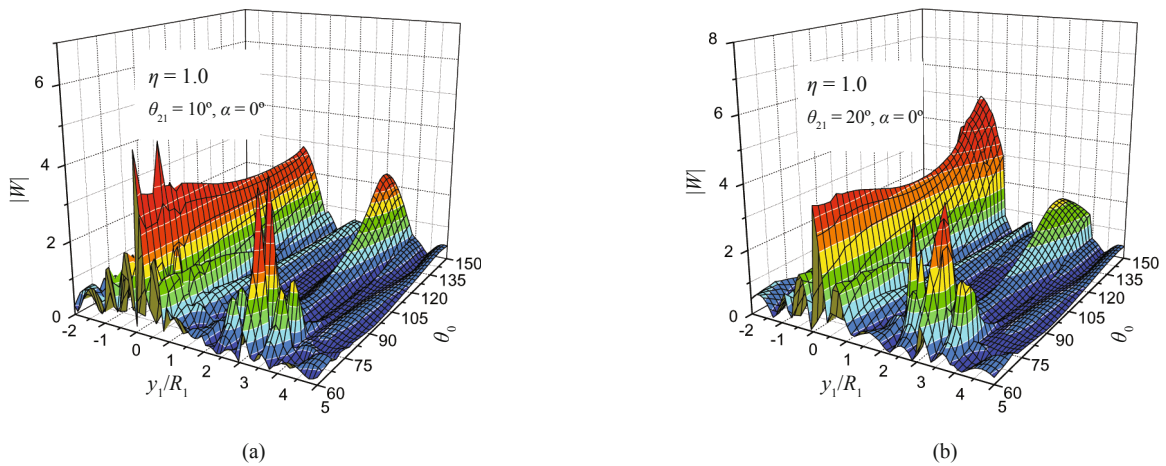


Fig. 9 Surface displacements

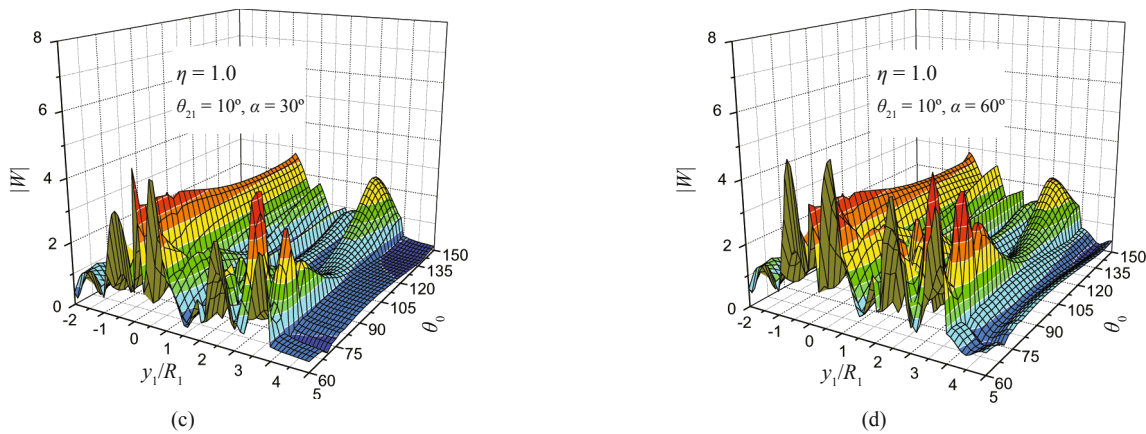


Fig. 9 Continued

8 Conclusions

(1) “Division” and “conjunction” technique are developed in this paper to analyze antiplane response of two scalene triangular hills and a semi-cylindrical canyon under incident SH-waves based on the methods of wave function expansion, complex function and multi-polar coordinates.

(2) Based on above numerical results, it can be concluded that the parameters of the incident wave such as wave number and incident angle have considerable influence on the surface displacement amplitudes of multiple scalene triangular hills and a semi-cylindrical canyon. The dynamic characteristic of ground motion is increasingly obvious when the frequency η rises. The valley value of surface displacements of the canyon always occurs at $y_1/R_1 \approx 1.5$ and increases by the increment of incident angle α when $\eta = 1.0$.

(3) When SH-waves are incident vertically into $X_1Y_1O_1$ coordinate plane, the maximum displacement amplitude $|W|_{\max}$ always occurs at $y_1/R_1 = \Delta_1$ (the vertex of the first triangular hill). Besides, the surface displacements nearby are impacted much more strongly by SH-waves than further field.

(4) The results in this paper can provide theory value for earthquake engineering and the methods used can be also branched out into the scattering problems of P-wave and SV-wave on multiple scalene triangular hills and semi-cylindrical canyons.

Acknowledgement

This study was supported by Natural Science Foundation of Heilongjiang Province, China under Grant No. A201310, and the Scientific Research Starting Foundation for Post Doctorate of Heilongjiang Province, China under Grant No. LBH-Q13040.

References

Cao XR, Song TS and Liu DK (2001), “Scattering

of Plane SH-wave by a Cylindrical Hill of Arbitrary Shape,” *Applied Mathematics and Mechanics* (English Edition), 22(9): 1082–1089.

Chang KH, Tsaur DH and Wang JH (2013), “Scattering of SH Waves by a Circular Sectorial Canyon,” *Geophysical Journal International*, 195(1): 532–543.

Chen JT, Lee JW, Wu CF and Chen IL (2011), “SH-wave Diffraction by a Semi-circular Hill Revisited: A Null-field Boundary Integral Equation Method Using Degenerate Kernels,” *Soil Dynamics and Earthquake Engineering*, 31(5–6): 729–736.

Cui ZG, Zou YC and Liu DK (1998), “Scattering of Plane SH-waves by a Cylindrical Hill of Circular-arc Cross Section,” *Earthquake Engineering and Engineering Vibration*, 18(4): 8–14. (in Chinese)

Du YJ, Liu DK, Zhao QC, Qiu FQ and Wang CH (2009), “Ground Motion of Isosceles Triangular and Semi-circular Hills with the SH Incident Wave,” *World Earthquake Engineering*, 25(3): 167–174. (in Chinese)

Lee VW and Alongkorn A (2013), “Scattering of Anti-plane (SH) Waves by a Semi-elliptical Hill: I—Shallow Hill,” *Soil Dynamics and Earthquake Engineering*, 52: 116–125.

Lee VW, Luo H and Liang JW (2004), “Diffraction of Anti-plane SH Waves by a Semi-circular Cylindrical Hill with an Inside Concentric Semi-circular Tunnel,” *Earthquake Engineering and Engineering Vibration*, 3(2): 249–262.

Li M, Liu DK and Zhou RF (2008), “Scattering of SH-waves by a Semi-cylindrical Hill with a Hole and Multiple Cavities around It in Half-space,” *Journal of Harbin Engineering University*, 29(1): 78–84. (in Chinese)

Liang JW, Zhang YS and Lee VW (2005), “Scattering of Plane P Waves by a Semi-cylindrical Hill: Analytical Solution,” *Earthquake Engineering and Engineering Vibration*, 4(1): 27–36.

Liu DK, Cao XR and Cui ZG (1998), “Scattering of Plane SH-waves by Semi-cylindrical Hills,” *ACTA*

- Mechanica Solida Sinica*, (Sup. 1): 178–185.
- Liu DK and Han F (1990), “Scattering of Plane SH-waves by Cylindrical Canyon of Arbitrary Shapes in Anisotropic Media,” *ACTA Mechanica Sinica*, **6**(3): 256–266.
- Liu DK and Wang GQ (2006), “Antiplane SH-deformation of a Semi-cylindrical Hill above a Subsurface Cavity,” *ACTA Mechanica Sinica*, **38**(2): 209–218.
- Liu G, Chen HT and Liu DK (2010), “Surface Motion of a Half-space with Triangular and Semicircular Hills under Incident SH Waves,” *Bulletin of the Seismological Society of America*, **100**(3): 1306–1319.
- Liu G and Liu DK (2007), “Ground Motion of an Isosceles Triangular Hill above a Subsurface Cavity with Incident SH Waves,” *Acta Mechanica Solida Sinica*, **28**(1): 60–66. (in Chinese)
- Liu HW and Liu DK (1997), “Scattering of P-waves by Canyons with Variable Depth-to-width Ratio,” *ACTA Mechanica Solida Sinica*, **18**(4): 295–300.
- Lu XT and Liu DK (2006), “Ground Motion of a Semicylindrical Hill and a Semi-cylindrical Canyon Caused by Incident SH Wave,” *Earthquake Engineering and Engineering Vibration*, **26**(5): 14–20. (in Chinese)
- Lu XT, Yang ZL and Liu DK (2009), “Antiplane Response of Multiple Semi-cylindrical Hills above a Subsurface Elastic Cylindrical Inclusion to Incident,” *World Earthquake Engineering*, **25**(2): 114–119. (in Chinese)
- Nazaret D, Lee VW and Liang JW (2003), “Antiplane Deformations around Arbitrary-shaped Canyons on a Wedge-shape Half Space: Moment Method Solutions,” *Earthquake Engineering and Engineering Vibration*, **2**(2): 281–287.
- Qi H, Guo J and Yang J (2012), “Scattering of SH-wave and Ground Motion Induced by Scalene Triangular Hill on a Right-angle Field,” *Journal of Vibration and Shock*, **31**(18): 157–162. (in Chinese)
- Qiu FQ and Liu DK (2005), “Antiplane Response of Isosceles Triangular Hill to Incident SH Waves,” *Earthquake Engineering and Engineering Vibration*, **4**(1): 37–46.
- Shyu WS and Teng TJ (2011), “SH Wave Scattering at a Trapezoid Hill and a Semi-cylindrical Alluvial Basin by Hybrid Method,” *2011 International Conference on Consumer Electronics, Communications and Networks*, 5215–5218.
- Trifunac MD (1992), “Surface Motion of a Semi-Cylindrical Alluvial Valley for Incident Plane SH Waves,” *Bull Seism Soc Am*, **61**(2): 1755–1770.
- Tsaur DH and Hsu MS (2013), “SH Waves Scattering from a Partially Filled Semi-elliptic Alluvial Valley,” *Geophysical Journal International*, **194**(1): 499–511.
- Yuan XM and Liao ZP (1996), “Scattering of Plane SH Waves by a Cylindrical Hill of Circular-arc Cross-section,” *Earthquake Engineering and Engineering Vibration*, **16**(2): 1–13. (in Chinese)
- Zhang N, Gao YF, Li DY, Wu YX and Zhang F (2012), “Scattering of SH Waves Induced by a Symmetrical V-shaped Canyon: a Unified Analytical Solution,” *Earthquake Engineering and Engineering Vibration*, **11**(4): 445–460.
- Zhang YS (2010), “Analytical Solution to Dynamic Response of Circular-arc-shaped Multi-layered Valley due to Incidence of Rayleigh Wave,” *Chinese Journal of Geophysics*, **53**(9): 2129–2143.(in Chinese)
- Zhang YS (2010), “Analytical Solution to Dynamic Response of Circular-arc-shaped Multi-layered Valley due to Incidence of Rayleigh Wave,” *Chinese Journal of Geophysics*, **53**(9): 2129–2143.(in Chinese)